

# BACK ANALYSIS OF LARGE GEOTECHNICAL MODELS

G. SWOBODA<sup>1,\*</sup>, Y. ICHIKAWA<sup>2</sup>, QINXI DONG<sup>1</sup> AND MOSTAFA ZAKI<sup>1</sup>

<sup>1</sup> *University of Innsbruck, Technikerstrasse 13, Innsbruck, Austria*

<sup>2</sup> *Nagoya University, Nagoya, Japan*

## SUMMARY

This paper gives a brief review, comparison and further development of back analysis procedures in geotechnical models. The dual boundary control method is adopted to develop a general back analysis code suitable for parameter identification of large, complex geotechnical problems. The procedure for parameter identification is discussed here for both 2D and 3D models. Some numerical examples were given to illustrate the applicability and the convergence of this procedure, with special care being taken for tunnel applications to ensure that the method is suitable for large systems. Copyright © 1999 John Wiley & Sons, Ltd.

KEY WORDS: finite elements; back analysis; tunneling; geomechanics; parameter identification

## 1. INTRODUCTION

Back analysis is a procedure for solving system identification (or ‘characterization’ or ‘calibration’) problems, where the unknown system is characterized via its response. The system is simulated in a model, and the input parameters of the model are identified through the output information. Synonym ‘back analysis’ well reflects the backward nature of this calibration procedure, and together with the basic concepts and methods of identification theory it was introduced to geotechnical engineering by Gioda and Sakurai,<sup>1</sup> Cividini<sup>2</sup> and their co-workers.

With regard to the natural origin and complex behaviour of geomaterials the back analysis procedures are of special importance to geotechnical engineering. Based on advanced measuring techniques and computer technology material properties, load distribution or geometric data can be back analysed using measured displacements or stresses of a geotechnical structure. The main fields of application are as follows:

1. Characterization of rock and soil parameters (deformation and strength characteristics) using field measurements in test galleries.<sup>3–5</sup>
2. Observational method for predicting the behaviour of a geotechnical structure by back analysing the measurements of an earlier stage of construction.<sup>6</sup>
3. Evaluation of rock and soil mechanics field tests.<sup>2,3,7</sup>
4. Calibration of laboratory tests.<sup>8,9</sup>

\*Correspondence to: G. Swoboda, Department of Structural Engineering, University of Innsbruck, Technikerstrasse 13, A-6020, Innsbruck, Austria. E-mail: swoboda@cgie.uibk.ac.at

Contract/grant sponsor: Austrian National Science Foundation; Contract/grant number: P10016

Contract/grant sponsor: Ministry of Education, Science and Culture of Japan; Contract/grant number: 06044096

With respect to classical stress analysis problems, the back analysis procedures in geomechanics used to be divided into two categories: the inverse and direct approaches.<sup>3,10</sup>

In the *inverse* approach, the system of equations governing the problem is rewritten in such a way that material parameters appear as unknowns and measured displacements or stresses as input data. The first inverse algorithm based on the Finite Element Method was proposed by Kavanagh and Clough,<sup>11</sup> but the first inverse approach applicable to parameter identification in geotechniques was developed by Gioda.<sup>4,10</sup> It is used to search for elastic material parameters  $B$  and  $G$  ( $B$ , bulk modulus;  $G$ , shear modulus) and can be modified to calculate the earth pressure acting on a tunnel lining. The inverse algorithm suggested by Sakurai and Takeuchi<sup>5</sup> makes it possible to compute Young's modulus together with the initial stress state. Poisson's ratio and the vertical initial stress are assumed as known. The Kalman filter algorithm<sup>23</sup> was incorporated into Gioda's inverse algorithm by Murakami and Hasegawa.<sup>13</sup> This probabilistic procedure allows us to use the measurement error information in the inverse calculation and to evaluate the influence of measurement error on the results of back analysis.<sup>14</sup> An inverse algorithm for identifying parameters of a non-linear hyperelastic solid was suggested by Iding *et al.*<sup>8</sup>

The *direct* approach employs the trial values of the unknown parameters as input data in the stress analysis algorithm, until the discrepancy between measurements and numerical results is minimized. This discrepancy is commonly expressed as the error function  $\varepsilon = \{\sum_i^n [u_i - u_i^*]^2\}^{1/2}$ , where  $n$  is the number of measurements in the sense of the least-squares method. In order to minimize this error function, which is highly non-linear, algorithms known as direct search methods are used in mathematical programming.<sup>15</sup> The Simplex method, the Rosenbrock algorithm and the Powell method were recommended for this purpose by Gioda.<sup>3,4,10</sup> The probabilistic Bayesian approach was incorporated into the direct algorithm by Cividini.<sup>16</sup> This approach permits us to make use of both the '*a priori*' information on the unknown parameters (experience, engineering judgement) and information on the measurement reliability, which are built into the objective function.

All the above methods have advantages and shortcomings. The advantages of the inverse algorithm are: smooth and fast convergence and stable behaviour, provided the measurement data set is well selected.<sup>10,17</sup> This is due to boundary control built in the algorithm. Points where both the nodal forces and nodal displacements are known basically control the error minimizing procedure. This ensures quick convergence for data of good quality, but can cause divergence of the procedure in the case of ill-selected measurement data.

Direct formulation is very flexible, and this approach is therefore, used to back-analyse parameters for more complex constitutive models, where the inverse relations cannot be derived in the simple direct way. Furthermore, development of the direct back analysis code is much less difficult than development of the code based on an inverse algorithm, because the Finite Element solution can be used in direct methods as part of the optimizing program without any changes. On the other hand, the course of convergence is highly dependent on the number of unknown parameters, the quality of their initial guess and on the optimization strategy chosen. Direct method gives an insufficient solution, especially in a case where Young's modulus and Poisson's ratio are identified simultaneously.

## 2. DUAL BOUNDARY CONTROL METHOD

The boundary control method suggested by Ichikawa,<sup>18</sup> combines the advantages of both approaches. In the inverse portion of this algorithm the equilibrium equation is coupled together

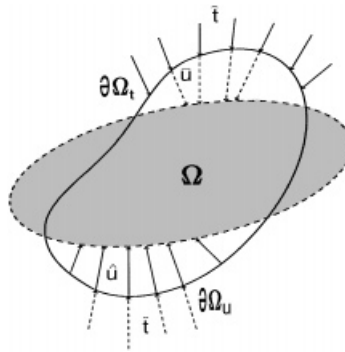


Figure 1. Boundary control model

with observational boundary conditions and the direct part of the algorithm improves convergence of the Newton iteration process.

The concept of the dual boundary control method, Figure 1, is based on separation of the domain  $\Omega$  in a dual system  $\Omega_t$ , with measured displacements  $\bar{U}$  and tractions  $\hat{t}$  due to the known loading, and the domain  $\Omega_u$  with measured tractions  $\bar{t}$  and corresponding displacements  $\hat{U}$ . Due to the problem of measuring traction, the boundary  $\Omega_t$  is not used in this formulation.

The virtual work of problem is

$$\int_{\Omega} \sigma : \delta \varepsilon \, dv - \int_{\partial \Omega_t} \hat{t} \cdot \delta u \, dS = 0 \quad (1)$$

where  $\sigma$  is the stress and  $\delta \varepsilon$  the virtual strain in the domain  $\Omega$ ,  $\hat{t}$  is the traction and  $\delta u$  is the virtual displacement in the boundary  $\partial \Omega_t$ .

The Finite Element Method can be applied to equation (1) for an approximate solution, which satisfies the equation

$$\mathbf{K} \mathbf{U} = \mathbf{F} \quad (2)$$

where

$$\mathbf{K} = \int_{\Omega} \mathbf{B}^T \mathbf{D} \mathbf{B} \, dv, \quad \mathbf{F} = \int_{\partial \Omega_t} \mathbf{N}^T \hat{t} \, dS$$

where  $\mathbf{N}$  is the matrix of shape functions,  $\mathbf{B}$  the strain-displacement matrix and  $\mathbf{D}$  the elastic stiffness matrix.

Equation (2) is expressed with the unknown material parameters  $P$  as follows:

$$\int_{\Omega} \mathbf{B}^T \mathbf{D}(P) \mathbf{B} \, dv \cdot \mathbf{U} = \mathbf{F} \quad (3)$$

namely

$$\mathbf{K}(P) \mathbf{U} = \mathbf{F} \quad (4)$$

The observed displacement boundary condition is defined as

$$\mathbf{S}_u \mathbf{U} = \bar{\mathbf{U}} \quad (5)$$

where  $S_u$  is the diagonal matrix.

### 3. SOLUTION TECHNIQUE FOR LARGE SYSTEMS

This problem can be solved with the help of optimization procedures, as shown by Dennis *et al.*<sup>19,23</sup> The problem can be formulated as a non-linear least-squares problem, in which we want to minimize the function

$$f(x) = \frac{1}{2} R(x)^T R(x) \quad (6)$$

The residual vector  $R(x)$  of equations (4) and (5) is expressed as follows:

$$R(x) = \begin{bmatrix} F - K(P)U \\ \bar{U} - S_u U \end{bmatrix} \triangleq \begin{Bmatrix} R_1 \\ R_2 \end{Bmatrix} \quad \text{with} \quad x = (U | P)^T \quad (7)$$

where  $x$  is the assembled vector of the unknown variables, the nodal displacements  $U$  and the material parameters  $P$ . In equation (7) the observed displacement is  $\bar{U}$ .

The Jacobian matrix of  $R(x)$  is  $J(x)$ , where  $J(x)_{ij} = \partial R_i / \partial x_j$ ,

$$J = \begin{bmatrix} \frac{\partial R_1}{\partial U} & \frac{\partial R_1}{\partial P} \\ \frac{\partial R_2}{\partial U} & \frac{\partial R_2}{\partial P} \end{bmatrix} = \begin{bmatrix} -K(P) & -\frac{\partial K}{\partial P} U \\ -S_u & 0 \end{bmatrix} \triangleq -G \quad (8)$$

We wish to find  $x^*$ , which minimizes  $f(x) = \frac{1}{2} R(x)^T R(x)$ . This can be solved with the Gauss–Newton approach using an affine model of  $R(x)$  close to  $x^k$ :

$$M_k(x) = R(x^k) + J(x^k)(x - x^k) = R_k - G_k dx \quad (9)$$

and seek to minimize

$$E_k(x) \triangleq \frac{1}{2} M_k(x)^T M_k(x) \quad (10)$$

The solution for iteration  $k + 1$  is as follows:

$$x^{k+1} = x^k - [J_k^T J_k]^{-1} J_k^T R_k \quad (11)$$

where

$$J_k = J(x_k), \quad R_k = R(x_k), \quad J = -G$$

By substituting  $J = -G$ , we get the solution for the next unknown parameter vector:

$$x^{k+1} = x^k + [G_k^T G_k]^{-1} G_k^T R_k \quad (12)$$

The incremental formulation

$$dx = x^{k+1} - x^k \quad (13)$$

can be written in the following form:

$$[G_k^T G_k] dx = G_k^T R_k \quad (14)$$

The finite element solution for equation (14) can be found by substituting equations (7) and (8). We thus obtain the formulation

$$\mathbf{G}^T \mathbf{G} = \left[ \begin{array}{cc} K^2 + S_u & K \left( \frac{\partial K}{\partial P} U \right) \\ \left( \frac{\partial K}{\partial P} U \right)^T K & \left( \frac{\partial K}{\partial P} U \right)^T \frac{\partial K}{\partial P} U \end{array} \right]^k \quad (15)$$

$$\mathbf{G}^T \mathbf{R} = \left\{ \begin{array}{c} K(F - KU) + \bar{U} - S_u U \\ \left( \frac{\partial K}{\partial P} U \right)^T (F - KU) \end{array} \right\}^k \quad (16)$$

In order to make use of the reliable equation solver available and to avoid forming  $K^2$  directly, a special equation solution scheme is applied. With the substitutions:

$$\mathbf{G}_{12} = K \left( \frac{\partial K}{\partial P} U \right), \quad \mathbf{G}_{22} = \left( \frac{\partial K}{\partial P} U \right)^T \frac{\partial K}{\partial P} U \quad (17)$$

$$\mathbf{Q}_1 = K(F - KU) + \bar{U} - S_u U, \quad \mathbf{Q}_2 = \left( \frac{\partial K}{\partial P} U \right)^T (F - KU) \quad (18)$$

the system equation (14) becomes

$$\left[ \begin{array}{cc} \mathbf{K}^2 + S_u & \mathbf{G}_{12} \\ \mathbf{G}_{12}^T & \mathbf{G}_{22} \end{array} \right] \left\{ \begin{array}{c} d\mathbf{U} \\ d\mathbf{P} \end{array} \right\} = \left\{ \begin{array}{c} \mathbf{Q}_1 \\ \mathbf{Q}_2 \end{array} \right\} \quad (19)$$

which is the explicit formulation of the parameter identification problem. The equation system is very similar to the finite element formulation; the element stiffness matrix  $\mathbf{K}$  needs only to be extended by the identification matrices  $\mathbf{G}_{12}$  and  $\mathbf{G}_{22}$ . Likewise, the load vector must be modified to  $\mathbf{Q}_1$  and  $\mathbf{Q}_2$ . To simplify the solution, equation (19) can be explicitly written as

$$(K^2 + S_u) dU + G_{12} dP = Q_1 \quad (20)$$

$$G_{12}^T dU + G_{22} dP = Q_2 \quad (21)$$

Equation (20) can be written as

$$dU = [K^2 + S_u]^{-1} (Q_1 - G_{12} dP) \quad (22)$$

Substituting it into equation (21) yields

$$(G_{22} - G_{12}^T [K^2 + S_u]^{-1} G_{12}) dP = Q_2 - G_{12}^T [K^2 + S_u]^{-1} Q_1 \quad (23)$$

In this procedure there is no need to calculate  $K^2$  or  $[K^2 + S_u]^{-1}$ . Multiplication of matrices like  $[K^2 + S_u]^{-1} R$ , where  $R$  is the vector of  $n \times 1$ , can be performed as follows. Suppose

$$[K^2 + S_u]^{-1} R = X \quad (24)$$

then we have

$$(K^2 + S_u)X = R \quad (25)$$

This can also be written in the form

$$K(KX) = R - S_u X \quad (26)$$

This equation for  $X$  can be solved with an iterative procedure. In the beginning, the initial  $X$  value on the right-hand side can be assumed to be  $\{0\}$ . Solving the equation by performing the back substitution twice, we obtain the next value for  $X$ . The calculation is continued until convergent. Considering the fact that the values for  $S_u$  are much smaller than those for  $K$ , convergence will be reached very soon.

Using equation (23) the unknown incremental parameters  $dP$  can be found. By substituting  $dP$  into equation (20), the equation for  $dU$  is obtained as

$$(K^2 + S_u)dU = Q_1 - G_{12}dP \quad (27)$$

Similarly, this equation can also be solved with the iterative procedure, as shown for equation (26), without calculating  $K^2$  or  $[K^2 + S_u]^{-1}$ .

The solution procedure for equation (19) is based on the conjugate gradient method proposed by Fletcher and Reeves,<sup>20</sup> which is applied during each iteration step  $k$ . For this procedure we introduce an error function, which is equal to the differences of the square of calculated displacements  $u_i$  and measured quantities  $\bar{u}_i$  for  $n$  measurements:

$$W(P) = \frac{1}{2} \sum_{i=1}^n (u_i - \bar{u}_i)^2 \quad (28)$$

The solution for the unknown parameters should be found under consideration of an upper limit  $P_{\max}$  and a lower limit  $P_{\min}$ :

$$P_{\min} < P < P_{\max} \quad (29)$$

The conjugate gradient methods using minimization of the function

$$W(P^k + \lambda dP^k) \rightarrow \min \quad (30)$$

determine the scalar  $\lambda$ . The solution procedures for step  $k$  can be executed using the following steps:

- (1) Select an initial value for the scalar  $\lambda$ .
- (2) Calculate the gradients  $g_l = \partial W(P)/\partial \lambda$ , where  $l$  is the iteration number to minimize the function  $W(P)$ .
- (3) Find the improvement of the solution for  $P$  for the  $l$ th iteration step using

$$P^{l+1} = P^l + \lambda_l S_l dP$$

where

$$S_l = -g_l + \frac{(g_l^T g_l)}{(g_{l-1}^T g_{l-1})} S_{l-1} \quad (31)$$

- (4) Find the scalar for the next iteration step  $\lambda_{l+1}$  according to Reference 20 by minimizing the objective function locally.
- (5) Check whether the convergence condition  $\|g_l\| < \varepsilon$  is satisfied. If not, steps (1)–(4) should be repeated.
- (6) After convergence the parameters can be defined for the next step  $k + 1$

$$P^{k+1} = P^k + \lambda dP^k \quad (32)$$

and then the displacements correspond to the  $P^{k+1}$  as follows:

$$U^{k+1} = U^k + \lambda dU^k \quad (33)$$

- (7) The convergence criterion for the step  $k + 1$  must satisfy the following conditions:

$$\frac{\|U^{k+1} - U^k\|}{\|U^{k+1}\|} < \varepsilon_1 \quad \text{and} \quad \frac{\|P^{k+1} - P^k\|}{\|P^{k+1}\|} < \varepsilon_2 \quad (34)$$

where the constants are in the limit  $0 < \varepsilon_1, \varepsilon_2 \ll 1$ .

#### 4. IDENTIFICATION OF VARIOUS MATERIALS

This method can be applied for various elements and materials in order to identify the various parameters such as  $E, v, G, \dots$  etc. This approach requires evaluation of the stiffness matrix derivative  $\partial K / \partial P$ , where  $P$  is the vector of unknown parameters. Matrix  $\partial K / \partial P$  is assembled in the same way as the stiffness matrix  $K$ , where  $\partial K_i^e / \partial P$  are element stiffness matrix derivatives over the different parameters such as  $E$  and  $v$ . These terms are obtained by numerical integration over the element volume  $V$

$$\frac{\partial K_i^e}{\partial P} = \int_{V_e} B^T \frac{\partial D}{\partial P} B dv \quad (35)$$

$D$  is introduced here due to the fact that only the  $D$  matrix is a function of material parameters.

##### 4.1. Joint parameters

Application of the theory is shown with the help of the joint elements as proposed by Goodman.<sup>12,21</sup> The four-node joint element JOINT with no thickness is shown in Figure 2. It models the contact plane with the help of the tangential and normal stiffness. In the joint the relation between stress and strain in the local coordinate system  $(s, n)$  is

$$\begin{Bmatrix} \tau_s \\ \sigma_n \end{Bmatrix} = \begin{bmatrix} \mathbf{k}_s & 0 \\ 0 & \mathbf{k}_n \end{bmatrix} \begin{Bmatrix} \Delta \mathbf{u}_s \\ \Delta v_n \end{Bmatrix} \quad (36)$$

where  $\tau_s$  and  $\sigma_n$  are the stress in the tangential and normal direction, respectively;  $\mathbf{k}_s$  and  $\mathbf{k}_n$  are the joint stiffness per unit length in the tangential and normal directions, respectively. The relative tangential and normal displacement of the corresponding points is  $\Delta \mathbf{u}_s$  and  $\Delta v_n$ .

With this equation (36), we can easily obtain the element stiffness  $K^e$  of the joint element. In order to obtain the identification matrices  $G_{12}$  and  $G_{22}$  and the load vectors  $Q_1$  and  $Q_2$ , we need the parameter derivative matrices  $\partial K^e / \partial k_s$  and  $\partial K^e / \partial k_n$ .

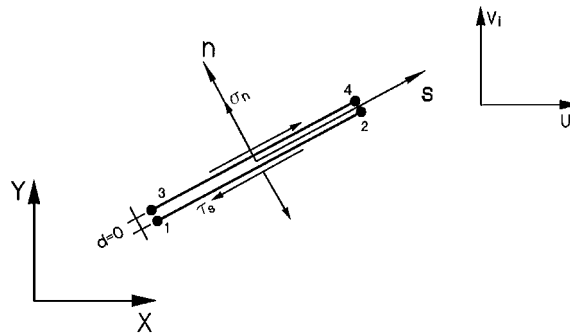


Figure 2. Joint element

$$\frac{\partial \mathbf{K}^e}{\partial \mathbf{k}_s} = \frac{1}{6} \begin{bmatrix} 2 & 0 & 1 & 0 & -1 & 0 & -2 & 0 \\ 0 & 0 & 0 & 0 & 0 & 0 & 0 & 0 \\ 1 & 0 & 2 & 0 & -2 & 0 & -1 & 0 \\ 0 & 0 & 0 & 0 & 0 & 0 & 0 & 0 \\ -1 & 0 & -2 & 0 & 2 & 0 & 1 & 0 \\ 0 & 0 & 0 & 0 & 0 & 0 & 0 & 0 \\ -2 & 0 & -1 & 0 & 1 & 0 & 2 & 0 \\ 0 & 0 & 0 & 0 & 0 & 0 & 0 & 0 \end{bmatrix} \quad (37)$$

$$\frac{\partial \mathbf{K}^e}{\partial \mathbf{k}_n} = \frac{1}{6} \begin{bmatrix} 0 & 0 & 0 & 0 & 0 & 0 & 0 & 0 \\ 0 & 2 & 0 & 1 & 0 & -1 & 0 & -2 \\ 0 & 0 & 0 & 0 & 0 & 0 & 0 & 0 \\ 0 & 1 & 0 & 2 & 0 & -2 & 0 & -1 \\ 0 & 0 & 0 & 0 & 0 & 0 & 0 & 0 \\ 0 & -1 & 0 & -2 & 0 & 2 & 0 & 1 \\ 0 & 0 & 0 & 0 & 0 & 0 & 0 & 0 \\ 0 & -2 & 0 & -1 & 0 & 1 & 0 & 2 \end{bmatrix} \quad (38)$$

Based on the solution of these derivate matrices (37) and (38), which must be formulated for any unknown parameter, the unknown identification matrices, equations (17) and (18), can be found.



#### 4.2. Isotropic materials in two-dimensional models

For two-dimensional elastic problems the dual boundary control method is applied with the help of the linearly varying strain triangular element LST.<sup>22</sup> Isotropic material is considered for plane stress and plane strain problems. In this case, two independent material constants, Young's modulus  $E$  and Poisson's ratio  $\nu$ , should be identified. Due to the fact that only  $D$  matrix is a function of the parameters  $E$  and  $\nu$ , we only have to find the matrices  $\partial D/\partial E$  and  $\partial D/\partial \nu$ .

The  $D$  matrix for plane stress is

$$D = \frac{E}{1 - \nu^2} \begin{bmatrix} 1 & \nu & 0 \\ \nu & 1 & 0 \\ 0 & 0 & (1 - \nu)/2 \end{bmatrix} \quad (39)$$

The  $D$  matrix for plane strain can be obtained from the plane stress condition by replacing  $E$  and  $\nu$  with  $E/(1 - \nu^2)$  and  $\nu/(1 - \nu)$ . We can obtain an equation similar to equation (39) for the plane strain problems. As examples, the matrices  $\partial D/\partial E$  and  $\partial D/\partial \nu$  for plane stress are given as follows:

$$\frac{\partial D}{\partial E} = \frac{1}{1 - \nu^2} \begin{bmatrix} 1 & \nu & 0 \\ \nu & 1 & 0 \\ 0 & 0 & (1 - \nu)/2 \end{bmatrix} \quad (40)$$

$$\frac{\partial D}{\partial \nu} = \frac{E}{(1 + \nu)^2} \begin{bmatrix} \frac{2\nu}{(1 - \nu)^2} & \frac{1 + \nu^2}{(1 - \nu)^2} & 0 \\ \frac{1 + \nu^2}{(1 - \nu)^2} & \frac{2\nu}{(1 - \nu)^2} & 0 \\ 0 & 0 & -\frac{1}{2} \end{bmatrix} \quad (41)$$

#### 4.3. Transverse isotropic materials of three-dimensional models

Application of the dual boundary control method is shown for isoparametric 20-nodes brick element. The elastic parameters  $E_1, E_2, G_2, \nu_1, \nu_2$  should be identified, which can be done with the help of general solution of the parameter identification problem (see [Reference 24] for details). Due to the fact that only the  $D$  matrix is a function of the parameters  $E_1, E_2, G_2, \nu_1$  and  $\nu_2$ . We only have to find the matrices  $\partial D/\partial E_1, \partial D/\partial E_2, \partial D/\partial G_2, \partial D/\partial \nu_1$  and  $\partial D/\partial \nu_2$ .

In the elasticity matrix  $D$  for transverse isotropic materials we can make the following changes  $n = E_1/E_2, m = G_2/E_2, p = 1 - \nu_1 - 2n\nu_2^2$  to obtain

$$D = \frac{E_2}{(1 + \nu_1)p} \begin{bmatrix} D_1 & D_2 & D_3 & 0 & 0 & 0 \\ D_2 & D_1 & D_3 & 0 & 0 & 0 \\ D_3 & D_3 & D_4 & 0 & 0 & 0 \\ 0 & 0 & 0 & D_5 & 0 & 0 \\ 0 & 0 & 0 & 0 & D_6 & 0 \\ 0 & 0 & 0 & 0 & 0 & D_6 \end{bmatrix} \quad (42)$$

where  $D_1 = n(1 - nv_2^2)$ ,  $D_2 = n(v_1 + nv_2^2)$ ,  $D_3 = nv_2(1 + v_1)$ ,  $D_4 = (1 - v_1^2)$ ,  $D_5 = 0.5np$ ,  $D_6 = m(1 + v_1)p$ .

In general, when the co-ordinate axes do not coincide with the principal axes of anisotropy, co-ordinate rotation is required. In such a case, the elasticity matrix  $D$  is determined from the following equation:

$$D = T_\sigma^T D_l T_\sigma \quad (43)$$

The matrix  $T_\sigma$  is the stress transformation matrix from the local reference  $x', y', z'$  co-ordinate system to the global  $x, y, z$  co-ordinate system (see [Reference 21]).

We find

$$\frac{\partial D}{\partial E_1} = \frac{1}{(1 + v_1)p^2} \begin{bmatrix} D_1 & D_2 & D_3 & 0 & 0 & 0 \\ D_2 & D_1 & D_3 & 0 & 0 & 0 \\ D_3 & D_3 & D_4 & 0 & 0 & 0 \\ 0 & 0 & 0 & D_5 & 0 & 0 \\ 0 & 0 & 0 & 0 & 0 & 0 \\ 0 & 0 & 0 & 0 & 0 & 0 \end{bmatrix} \quad (44)$$

where  $D_1 = (1 - v_1)(1 - 2nv_2^2) + 2n^2v_2^4$ ,  $D_2 = (1 - v_1)(v_1 + 2nv_2^2) - 2n^2v_2^4$ ,  $D_3 = (1 - v_1^2)v_2$ ,  $D_4 = 2(1 - v_1^2)v_2^2$ ,  $D_5 = 0.5p^2$ ,

$$\frac{\partial D}{\partial E_2} = \frac{1}{(1 + v_1)p^2} \begin{bmatrix} D_1 & D_1 & D_2 & 0 & 0 & 0 \\ D_1 & D_1 & D_2 & 0 & 0 & 0 \\ D_2 & D_2 & D_3 & 0 & 0 & 0 \\ 0 & 0 & 0 & 0 & 0 & 0 \\ 0 & 0 & 0 & 0 & 0 & 0 \\ 0 & 0 & 0 & 0 & 0 & 0 \end{bmatrix} \quad (45)$$

where  $D_1 = -(1 + v_1)n^2v_2^2$ ,  $D_2 = -2(1 + v_1)n^2v_2^3$ ,  $D_3 = (1 - v_1^2)(p - 2nv_2^2)$

$$\frac{\partial D}{\partial G_2} = \begin{bmatrix} 0 & 0 & 0 & 0 & 0 & 0 \\ 0 & 0 & 0 & 0 & 0 & 0 \\ 0 & 0 & 0 & 0 & 0 & 0 \\ 0 & 0 & 0 & 0 & 0 & 0 \\ 0 & 0 & 0 & 0 & 1 & 0 \\ 0 & 0 & 0 & 0 & 0 & 1 \end{bmatrix} \quad (46)$$

$$\frac{\partial D}{\partial v_1} = \frac{E_1}{(1 + v_1)^2 p^2} \begin{bmatrix} D_1 & D_2 & D_3 & 0 & 0 & 0 \\ D_2 & D_1 & D_3 & 0 & 0 & 0 \\ D_3 & D_3 & D_4 & 0 & 0 & 0 \\ 0 & 0 & 0 & D_5 & 0 & 0 \\ 0 & 0 & 0 & 0 & 0 & 0 \\ 0 & 0 & 0 & 0 & 0 & 0 \end{bmatrix} \quad (47)$$

where  $D_1 = 2(v_1 + nv_2^2)(1 - nv_2^2)$ ,  $D_2 = (1 + v_1)p - 2(v_1 + nv_2^2)^2$ ,  $D_3 = (1 + v_1)^2 v_2$ ,  $D_4 = 2(1 + v_1)^2 v_2^2$ ,  $D_5 = -0.5p^2$ ,

$$\frac{\partial D}{\partial v_2} = \frac{E_1}{(1 + v_1)p^2} \begin{bmatrix} D_1 & D_1 & D_2 & 0 & 0 & 0 \\ D_1 & D_1 & D_2 & 0 & 0 & 0 \\ D_2 & D_2 & D_3 & 0 & 0 & 0 \\ 0 & 0 & 0 & 0 & 0 & 0 \\ 0 & 0 & 0 & 0 & 0 & 0 \\ 0 & 0 & 0 & 0 & 0 & 0 \end{bmatrix} \quad (48)$$

where  $D_1 = 2n(1 + v_1)v_2$ ,  $D_2 = (1 + v_1)(p + 4nv_2^2)$ ,  $D_3 = 4(1 - v_1^2)v_2$ .

## 5. NUMERICAL EXAMPLES

The identification procedure is checked with the help of the back analysis of a Finite Element Model. This means that a selected number of displacements of the Finite Element Solution are the 'measured displacements' for the identification procedure.

### 5.1. Shear test

A system of two blocks will be analysed. The finite element idealization and measurement positions are shown in Figure 3(a). The two blocks are modelled by linearly varying strain triangular elements (LST element) and the interface by joint elements. The blocks are supposedly made of mortar, whose material properties are  $E = 2.5 \times 10^4$  MPa and  $v = 0.20$ . The material properties of the interface should be  $k_s = 1.0 \times 10^4$  MPa and  $k_n = 2.5 \times 10^4$  MPa. In this test the tangential stiffness  $k_s$  and normal stiffness  $k_n$  of the interface and Young's modulus  $E$  and Poisson's ratio  $v$  of the two blocks will be identified simultaneously using the identification procedure.

It is assumed that the vertical displacements at the end of the block and the horizontal displacement of the numerical test are 'measured' to see if the shear parameter  $k_s$ ,  $k_n$  and the elastic constants  $E$  and  $v$  of the blocks can be found at the same time. The converging processes of identification of all parameters are shown in Figure 3(b). The exact value is found after two and three iterations.

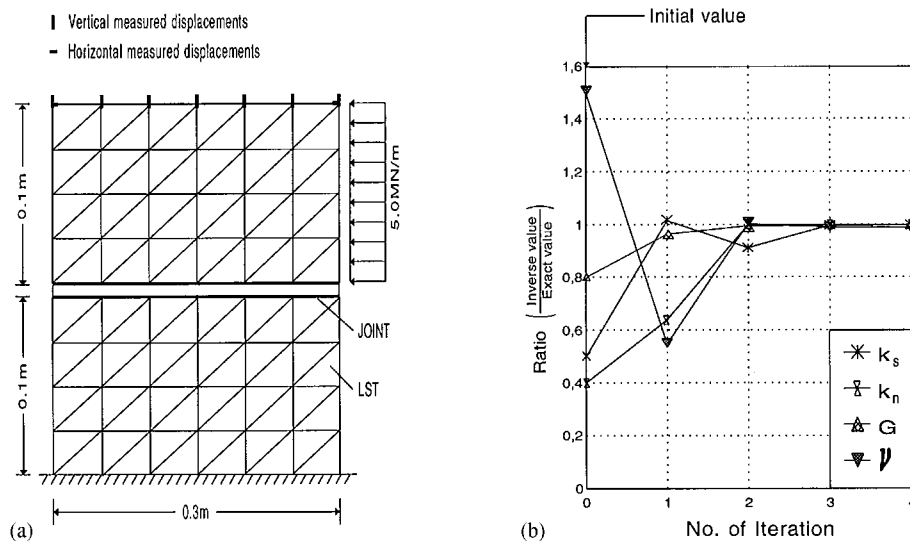


Figure 3. Shear test: (a) Finite element model; (b) iteration procedures of elastic constants

### 5.2. Two-layer system (variation of measured points)

The system is supposedly made of concrete with two different qualities. The material parameters are  $E_1 = 1.25 \times 10^7 \text{ kN/m}^2$ ,  $E_2 = 2.25 \times 10^7 \text{ kN/m}^2$  and Poisson's ratio for both layers is  $\nu = 0.20$ . The finite element idealization is shown in Figure 4, where the system is modelled by using 64 LST elements. The values of  $E_1$ ,  $E_2$  and  $\nu$  must be obtained and the convergence of the method checked.

With the help of this system three effects should be investigated. If we measure displacements only at the top of this system, it is assumed that any combination of material parameters will provide the same displacements. Figure 4 is a typical example with non-unique solution.

To show how the good choice of type and location of measured points affects the convergence and accuracy of the method, the measured points are moved from the top to the bottom of the system.

It should be noticed, due to equation (19), that the minimum required number of observations is equal to the number of unknown parameters, which is three in this case. On the choice of these measurements, it was found that observations of a symmetrical nature are not recommended as seen in Figure 4. No convergence was found for any selected position of the measured points. Whereas good convergence and identical parameter results with true values are obtained by choosing the measured points as in Figure 5, it is important from a practical point of view to notice that we can obtain the material parameters of the second layer without any measurement taken within this layer and *vice versa*. Due to the fact that this example is a continuum problem, the displacements are coupled. Thus, only a unique solution can be found.

### 5.3. Transverse isotropic material for three-dimensional models

In order to simulate driving of a tunnel, a three-dimensional model is selected.<sup>25</sup> The finite element model of this tunnel was based on the mesh shown in Figure 6. The soil around the tunnel

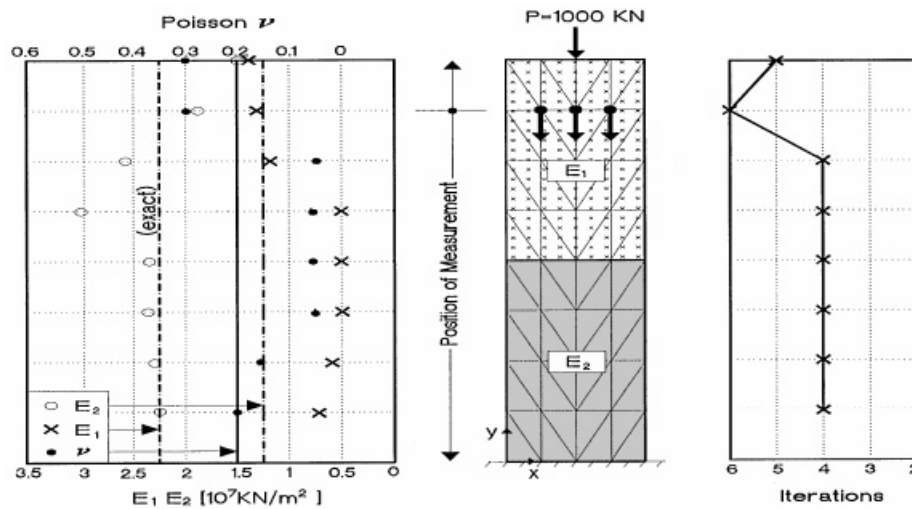


Figure 4. Two-layer system (with symmetrical measurements)

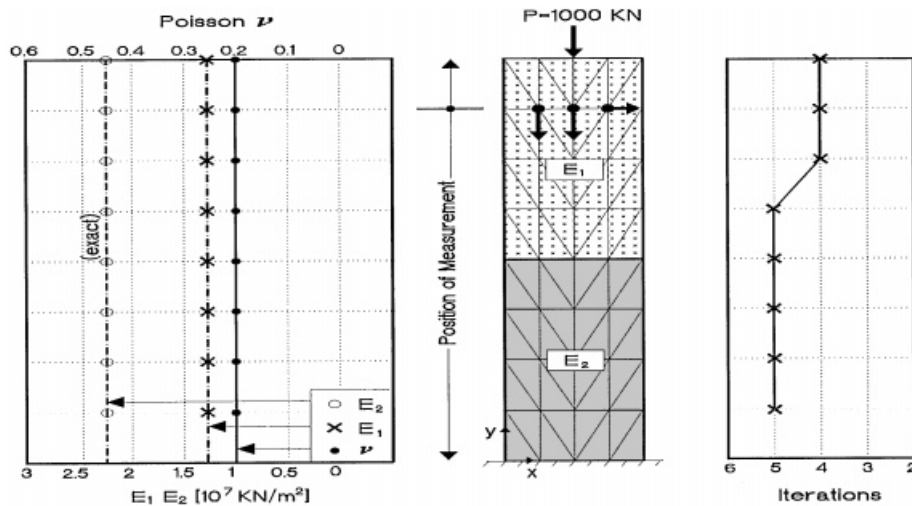


Figure 5. Two-layer system (with unsymmetrical measurements)

was simulated with 20-node brick elements, and the linings were simulated with 8-node shell elements. The finite element model has 336 brick elements and 48 shell elements, which resulted in a total of 1745 nodes and 5581 equilibrium equations. It is assumed that the initial stress field is known; the excavation process is divided into six loading steps for simulation of the stress redistribution due to excavation. The measurement points, for which vertical displacements were measured in section MS1 after four loading steps for two-layer transverse isotropic materials, are shown in Figure 7.

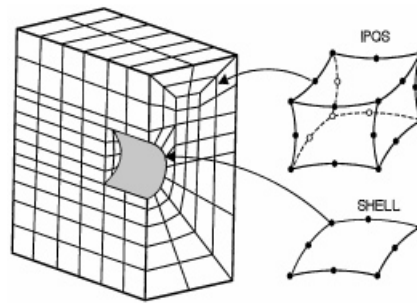


Figure 6. Finite element mesh for three-dimensional analysis

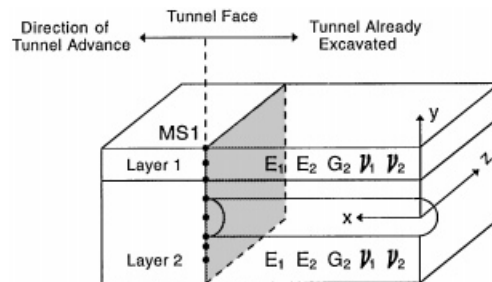


Figure 7. Position of the observed points

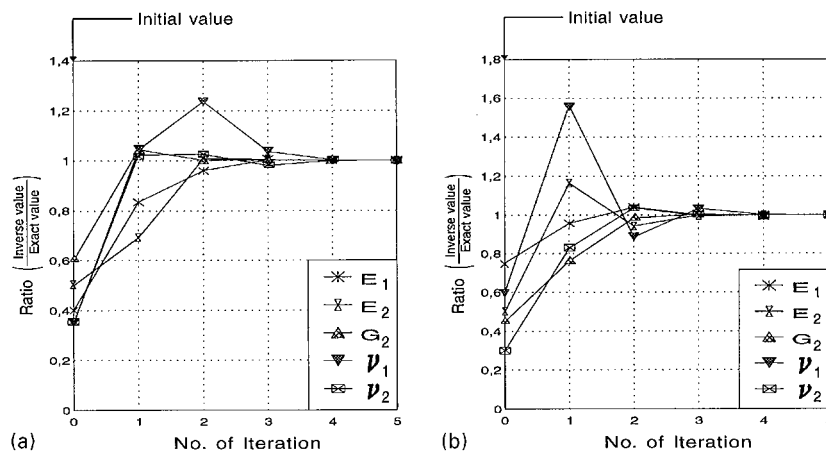


Figure 8. Iteration procedure for elastic constants: (a) First layer; (b) second layer

The parameters to be identified are  $E_1$ ,  $E_2$ ,  $G_2$  and  $\nu_1$ ,  $\nu_2$ . Convergence of the identification procedure is shown in Figure 8 for a two-layer model of transverse isotropic materials. Convergence is reached after five iteration steps for the first and second layer each. For the same model, numerical simulation is performed for the case that the parameters to be identified are only the

elastic moduli  $E_1$ ,  $E_2$ ,  $G_2$ . In this case convergence is achieved after three iteration steps for two layers. The impact of the initial values is not very high, so convergence could also be achieved for any selected starting value.

## 6. TUNNEL APPLICATION

The elastic parameters are to be identified for a subway tunnel<sup>26</sup> with a small height of overburden. For this tunnel the vertical and horizontal displacements are measured with an extensive site investigation program. The finite element model has 2435 nodes, 1143 triangular elements LST and 42 beam elements BEAM6. The measurement points are shown in Figure 9 and the measurements of various positions in the tunnel construction are listed in Table I. It is assumed that the initial stress field is known. The elastic constant  $E$  and Poisson's ratio  $\nu$  must be identified. To control the iteration process for Poisson's ratio a lower limit of 0.1 and an upper limit of 0.45 are selected. Two types of parameter identification calculation were performed. For case 1 only the vertical displacements observed and for case 2 the vertical and horizontal displacements are considered.

Table II shows the identified values in each case. Convergence is found after four iterations for case 1. For case 2 iteration stops after three steps, because the given lower limit of  $\nu$  is reached. But Figure 10(b) shows that the calculated displacements are still far from the measured displacements. This means a better result can only be found with anisotropic material. Good agreement can be found for the vertical displacements, as shown in Figure 10(a).

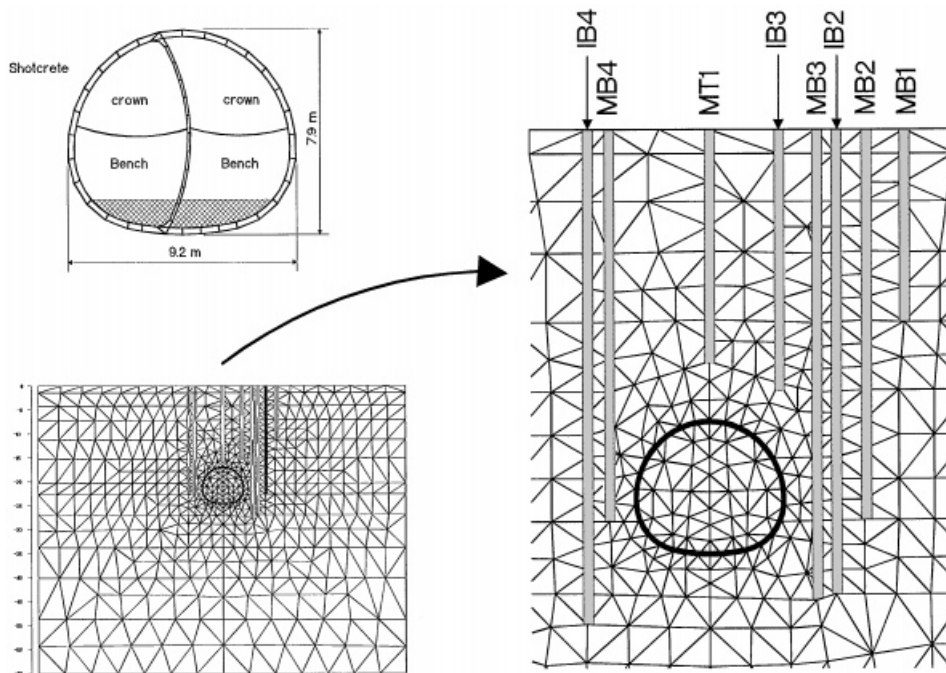


Figure 9. Position of the measurement system in the FEM mesh

Table I. Measurement program

Measurements	Positions							
	MB1	MB2	MB3	MT1	MB4	IB2	IB3	IB4
Horizontal						•	•	•
Vertical	•	•	•	•	•			

Table II. Identified results of tunnel model

	Initial	Case 1	Case 2
$E$ (MPa)	2.0	31.641	31.678
$\nu$	0.1	0.33558	—
No. of iterations		4	3

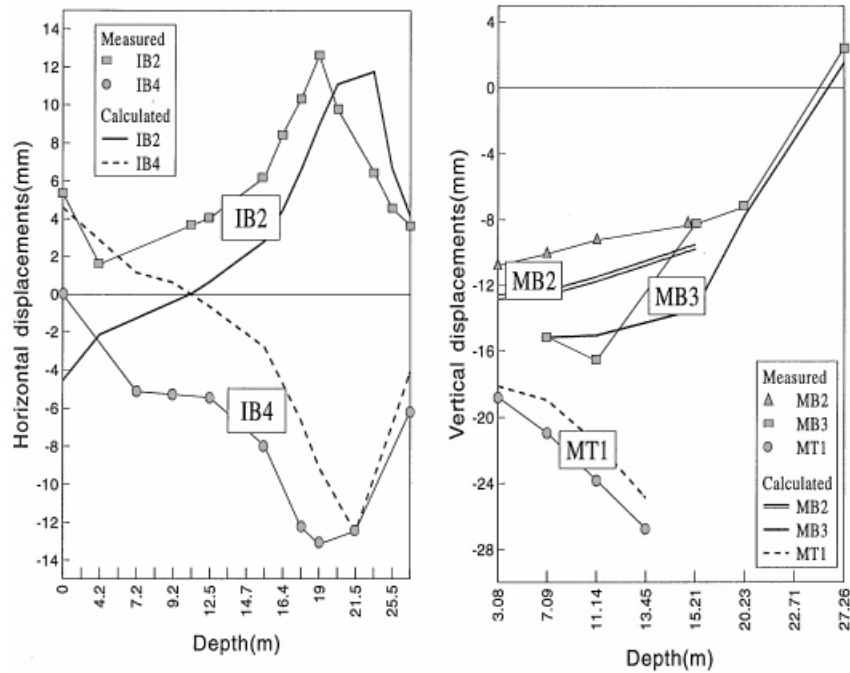


Figure 10. Comparisons between measured and calculated displacements

## 7. CONCLUSION

The identification procedure for elastic constants is performed for both 2D and 3D tunnel excavation problems. It has been shown that convergence is very fast. Convergence, however, does not mainly depend on the initial value of the parameters when the measurement points are



well selected. A well-chosen number and location of measurements provide accurate parameter results and good convergence, especially when simulating the moduli of elasticity and Poisson's ratio simultaneously.

### ACKNOWLEDGEMENTS

The work reported herein was performed under contract No. P10016 for 'Parameter Identification', which was supported by the Austrian National Science Foundation (Fonds zur Förderung der Wissenschaften), and under project No. 06044096, which was supported by the Ministry of Education, Science and Culture of Japan.

### REFERENCES

1. G. Gioda and S. Sakurai, 'Back analysis procedures for the interpretation of field measurements in geomechanics', *Int. J. Numer. Anal. Meth. Geomech.*, **11**(6), 555–583 (1987).
2. A. Cividini, L. Jurina and G. Gioda, 'Some aspects of characterization problems in geomechanics', *Int. J. Rock Mech. Mining Sci. Geomech. Abstr.*, **18**, 487–503 (1981).
3. G. Gioda and G. Maier, 'Direct search solution of an inverse problem in elastoplasticity: identification of cohesion, friction angle and *in situ* stress by pressure tunnel tests', *Int. J. Numer. Methods Engng.*, **15**, 1832–1848 (1980).
4. G. Gioda, 'Indirect identification of the average elastic characteristics of rock masses', *Int. Conf. on Structure and Foundation on Rock*, Sydney, 1980, pp. 65–73.
5. S. Sakurai and K. Takeuchi, 'Back analysis of measured displacements of tunnels', *Rock Mech. Rock Engng.*, **16**, 173–180 (1983).
6. A. Asaoka and M. Matsuo, 'An inverse problem approach to the prediction of multi-dimensional consolidation behaviour', *Soils Found.*, **24**, 49–62 (1984).
7. P. Berzi, 'Pile–soil interaction due to static and dynamic load', *13th ISSMFE*, New Delhi, 1994, pp. 609–612.
8. R. H. Iding, K. S. Pister and R. L. Taylor, 'Identification of nonlinear elastic solids by a finite element method', *Comput. Methods Appl. Mech. Engng.*, **4**, 121–142 (1974).
9. E. Imre, 'Model validation for the oedometric relaxation test', *13th ISSMFE*, New Delhi, 1994, pp. 1123–1126.
10. G. Gioda, 'Some remarks on back analysis and characterisation problems in geomechanics', *5th Int. Conf. on Numerical Methods in Geomechanics*, Nagoya, 1985, pp. 47–61.
11. K. I. Kavanagh and R. W. Clough, 'Finite element application in the characterization of elastic solid', *Int. J. Solids Struct.*, **7**, 11–23 (1971).
12. R. E. Goodman, R. L. Taylor and T. L. Brekke, 'A model for the mechanics of jointed rock', *Soil Mech. Found. Div.* **94**(SM3), 637–648 (1968).
13. A. Murakami and T. Hasegawa, 'Back analysis by kalman filter-finite elements and optimal location of observed points', *Proc. 22nd Japan National Conf. on Soil Mechanics and Foundation Engng.*, **2**, 1033–1036 (1987).
14. A. Ladesma, A. Gens and E. E. Alonso, 'Identification of parameters of nonlinear geotechnical models', in *Computer Methods and Advances in Geomechanics*, Balkema, Rotterdam, 1991, pp. 1005–1010.
15. M. J. Box, D. Davies and W. H. Swann, *Non-Linear Optimization Techniques*, Oliver and Boyd, Edinburgh, 1969.
16. A. Cividini, G. Maier and A. Nappi, 'Parameter estimation of a static geotechnical model using bayes approach', *Int. J. Rock Mech. Mining Sci.*, **20**, 215–226 (1983).
17. P. Venclik, 'Development of an inverse back analysis code and its verification', in *Numerical Methods in Geotechnical Engineering*, Balkema, Rotterdam, 1994, pp. 423–430.
18. Y. Ichikawa and T. Ohkami, 'A parameter identification procedure as a dual boundary control problem for linear elastic materials', *Soils Found.*, **32**, 35–44 (1992).
19. J. E. Dennis, J. R. Robert and B. Schnabel, *Numerical method for Unconstrained Optimization and Nonlinear Equations*, Prentice-Hall, Englewood Cliffs, N.J., 1983.
20. C. M. Fletcher and R. Reeves, 'Function minimization by conjugate gradient', *Comput. J.*, **7**, 149–154 (1964).
21. G. N. Pande, G. Beer and J. R. Williams, *Numerical Methods in Rock Mechanics*, Wiley, U.K., 1990.
22. K. Moser and G. Swoboda, 'Explicit stiffness matrix of the linearly varying strain triangular element', *Int. J. Comput. Struct.*, **8**, 311–314 (1978).
23. A. Murakami 'Studies on the application of kalman filtering to some geomechanical problems related to safety assessment', *Ph.D. Thesis*, Kyoto University, Japan.

24. G. Swoboda, Y. Tang and P. Venclik, 'Improvement of parameter identification procedures for large numerical models', *Proc. Int. Workshop*, Nagoya, 1994, pp. 107–136.
25. G. Swoboda, Q. Dong, M. Dolezalova and P. Venclik, Back analysis of three dimensional model for geotechnical problems, *Proc. Comput. Meth. Appl Sci.* '96, Paris, 1996, pp. 205–210.
26. G. Sauer, K. Zeidler and M. Marenče, *New Austrian Tunnelling Method applied in London Clay*, Geotechnical Engineering in Transportation Projects, Novigrad, Croatia, 1994.